Ballistic Impacts of a Full-Metal Jacketed (FMJ) Bullet on a Validated Finite Element (FE) Model of Helmet-Cushion-Head

*** Kwong Ming Tse[1], Long Bin Tan[1], Bin Yang[2], Vincent Beng Chye Tan[1], Siak Piang Lim[1,3], * Heow Pueh Lee[1,3]**

[1] Department of Mechanical Engineering, National University of Singapore
9 Engineering Drive 1, Singapore 117576
[2] College of Automobile and Traffic Engineering, Nanjing Forestry University
159 LongPan Rd, Nanjing, People's Republic of China 210037
[3] National University of Singapore (Suzhou) Research Institute
377 Lin Quan Street, Suzhou Industrial Park, Jiang Su
People's Republic of China 215123
*Corresponding author: tsekm@nus.edu.sg or tsekm.research@yahoo.com (Tse, K.M.);
mpeleehp@nus.edu.sg (Lee, H.P.)

Abstract

In order to determine the severity of the head injuries sustained from ballistic impact orientation and to investigate the effectiveness of the cushioned combat helmet in protecting the head from ballistic impact, series of ballistic impact simulations (frontal, lateral, rear and top) of FMJ bullet on a subject-specific FE head model, which are based on National Institute of Justice (NIJ) test standard. Two different designs of helmet interior cushion, namely the strap-netting system and the Oregon Aero (OA) foam, are adopted in this study. In general, the head experiences highest G in rear impacts among all impact orientations. The FE simulations also show that the use of OA foams helps to reduce frontal impact G forces and thus offers better protection from all various impact orientations. The OA cellular foams are more effective in limiting the transmission of force by being able to absorb more energy, via plateau characteristic prior to foam densification, compared to the stiffer linear elastic front cushion of strap-netted helmet. The simulations also showed both the helmets passed the NIJ requirement, WSTC and FMVSS criterion.

Keywords: Ballistic impact, helmet, subject-specific head model, head injury, cushion, head acceleration

1. Introduction

Advanced combat helmets (ACH) protects military personnel from sustaining traumatic brain injuries (TBI) due to blunt and ballistic impacts in both peace and war times. It is particularly important that these helmets are capable and effective in their function. Since 1970s, tremendous efforts had been spent on research of head protective helmets using finite element method (FEM) which serves as a cost-effective alternative to experiments [Khalil (1973; 1974); Van Hoof et al. (1999; 2001); Baumgartner and Willinger (2003); Aare and Kleiven (2007); Tham et al. (2008); Lee and Gong (2010); Yang and Dai (2010)] . For example, Khalil et al. (1974) performed low-velocity ballistic impacts using a very simplified head-helmet finite element (FE) model and validated against corresponding experiments. Van Hoof et al. (1999, 2001) found that the helmet interior exhibited large deformation exceeding the gap between inner helmet shell and head in experimental and numerical ballistic impact studies. Another study simulating ballistic impact on military helmet was by Baumgartner and Willinger (2003) who predicted skull fracture without traumatic brain injury (TBI). More recently, Aare and Kleiven (2007) studied the effects of helmet shell stiffness and impact orientation on a FE head model during a ballistic impact, while Yang and Dai (2010) focused on evaluation of the rear effect with different impact orientation. Of late, Tan et al. (2012) had performed both experimental tests and FE simulations on helmeted Hybrid III headform using

spherical projectile and found that foam cushioning system would help to reduce the head acceleration.
In order to determine the severity of the head injuries sustained from ballistic impact and to investigate the effectiveness of the cushioned combat helmet in protecting the head from ballistic impact, series of ballistic impact simulations (frontal, lateral, rear and top) of FMJ bullet on a subject-specific FEHM, which are based on National Institute of Justice (NIJ) test standard, were performed for a duration of 4ms using the explicit code in Abaqus v6.10 (SIMULIA, RI, USA). Similar to Tan et al. (2012), the interior cushioning systems included in this current study were namely strap-netting system (in Helmet 1) and Oregon Aero (OA) interior foam cushioning system (in Helmet 2). It should be noted that this subject-specific FEHM used in this study has been validated against the ICP and relative displacement data of three cadaveric experiments [Tse et al. (2014)].

2. Methods and Materials

2.1 Model Development and Model Description
The subject-specific FE model of human head and brain was reconstructed from computed tomography (CT) and magnetic resonance imaging (MRI) images. More details on the head model could be found in Tse et al. (2014)'s study. As for the advanced combat helmet (ACH) model, it was reconstructed from axial CT images while the two interior cushioning systems (OA foam and strap-netting) were drawn from scratch. The 9mm full-metal jacketed (FMJ) bullet, which geometrical details could be found in Tham et al. (2008)'s study, was used in the NIJ ballistic simulations. The entire assembly of the helmet-cushion-head model was shown in Figure 1. It should be noted that a preloading step was implemented prior to the actual ballistic impact step so that the two interior cushioning systems fit well with both the head and helmet models.

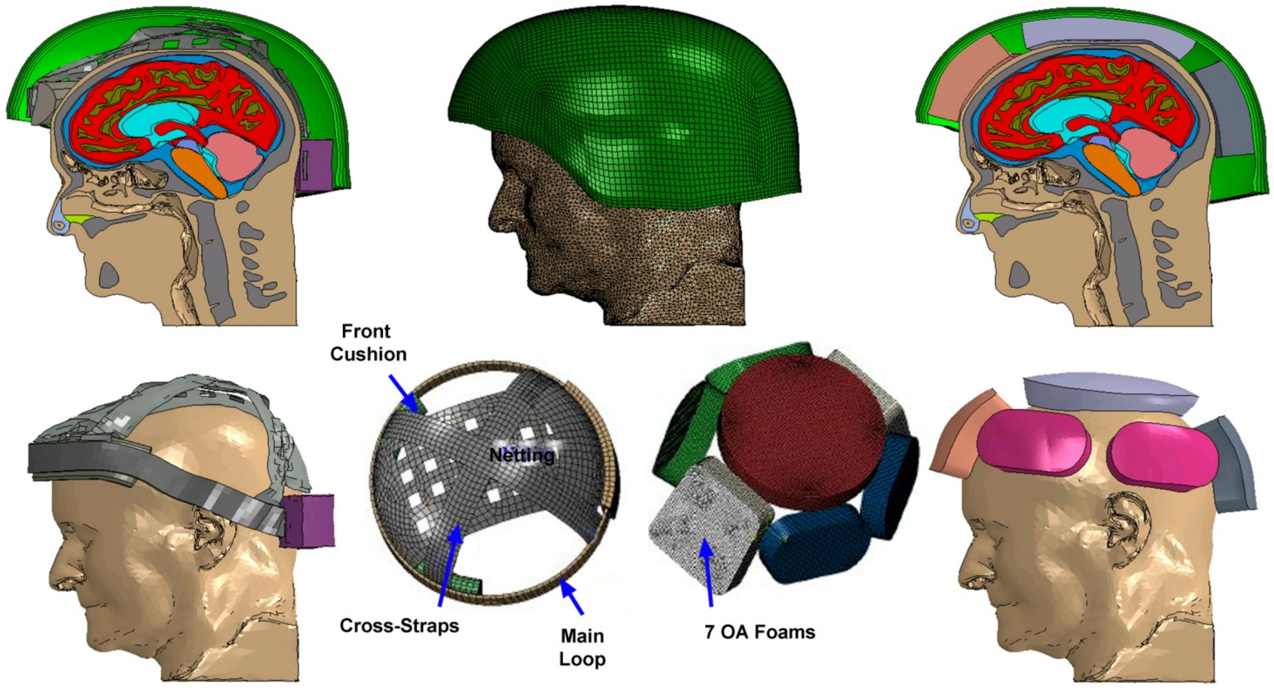

Figure 1: The two configurations of the helmet-interior cuhsion-head assembly.

2.2 Material Properties
For the head model, all the skeletal and cartilaginous tissues were modeled as linear elastic, isotropic materials, while the brain tissues were modeled with viscoelastic material properties [Tse et al. (2014)]. The helmet laminates adopted linear elastic but anisotropic material properties [Tan et

al. (2012)]. As for the two interior cushioning systems, their material properties were obtained from the in-house experiments in our previous work [Tan et al. (2012)]. The FMJ bullet, which is made of brass and lead, has its mechanical properties shown in Table 1.

Table 1: Material properties of both the intracranial and extracranial components used in the models.

<table>
<tr><th rowspan="2"></th><th rowspan="2">Components</th><th colspan="8">Material Properties</th></tr>
<tr><th colspan="5">Young's Modulus, E (MPa) / Shear Modulus, G (MPa)
$G(t) = G_\infty + (G_0 - G_\infty)e^{-\beta t}$</th><th colspan="2">Poisson's ratio, υ</th><th>Density, ρ (kg/mm^3)</th></tr>
<tr><td rowspan="14">Head</td><td>Brainstem</td><td colspan="5">G_0 = 0.0225 MPa, G_∞ = 0.0045 MPa, β = 80 s^{-1}</td><td colspan="2">0.4996</td><td>1.06E-06</td></tr>
<tr><td>Cerebral Peduncle</td><td colspan="5">G_0 = 0.0225 MPa, G_∞ = 0.0045 MPa, β = 80 s^{-1}</td><td colspan="2">0.4996</td><td>1.06E-06</td></tr>
<tr><td>Cerebrum</td><td colspan="5">G_0 = 0.528 MPa, G_∞ = 0.168 MPa, β = 35 s^{-1}</td><td colspan="2">0.48</td><td>1.14E-06</td></tr>
<tr><td>Cerebellum</td><td colspan="5">G_0 = 0.528 MPa, G_∞ = 0.168 MPa, β = 35 s^{-1}</td><td colspan="2">0.48</td><td>1.14E-06</td></tr>
<tr><td>CSF</td><td colspan="5">E = 1.314</td><td colspan="2">0.4999</td><td>1.04E-06</td></tr>
<tr><td>Gray Matter</td><td colspan="5">G_0 = 0.034 MPa, G_∞ = 0.0064 MPa, β = 700 s^{-1}</td><td colspan="2">0.4996</td><td>1.04E-06</td></tr>
<tr><td>Lateral Cartilage</td><td colspan="5">E = 30</td><td colspan="2">0.45</td><td>1.50E-06</td></tr>
<tr><td>Septum Cartilage</td><td colspan="5">E = 9</td><td colspan="2">0.32</td><td>1.50E-06</td></tr>
<tr><td>Bone</td><td colspan="5">E = 8000</td><td colspan="2">0.22</td><td>1.21E-06</td></tr>
<tr><td>Soft Tissues</td><td colspan="5">E = 16.7</td><td colspan="2">0.46</td><td>1.04E-06</td></tr>
<tr><td>Tooth</td><td colspan="5">E = 2070</td><td colspan="2">0.3</td><td>2.25E-06</td></tr>
<tr><td>Ventricles</td><td colspan="5">E = 1.314</td><td colspan="2">0.4999</td><td>1.04E-06</td></tr>
<tr><td>White Matter</td><td colspan="5">G_0 = 0.041 MPa, G_∞ = 0.0078 MPa, β = 700 s^{-1}</td><td colspan="2">0.4996</td><td>1.04E-06</td></tr>
<tr><td></td><td>E_{11} (MPa)</td><td>E_{22} (MPa)</td><td>E_{33} (MPa)</td><td>G_{12} (MPa)</td><td>G_{13}/G_{23} (MPa)</td><td>υ_{12}</td><td>$\upsilon_{13}/\upsilon_{23}$</td><td>ρ (kg/mm^3)</td></tr>
<tr><td>ACH</td><td>Helmet Shells</td><td>18000</td><td>18000</td><td>4500</td><td>770</td><td>2600</td><td>0.25</td><td>0.33</td><td>1230</td></tr>
<tr><td rowspan="6">Interior Cushion Systems</td><td>Cross Straps (Helmet 1)</td><td colspan="5">E = 60</td><td colspan="2">0.25</td><td>400</td></tr>
<tr><td>Front Cushion (Helmet 1)</td><td colspan="5">E = 18</td><td colspan="2">0.25</td><td>200</td></tr>
<tr><td>Main Loop (Helmet 1)</td><td colspan="5">E = 60</td><td colspan="2">0.25</td><td>400</td></tr>
<tr><td>Netting (Helmet 1)</td><td colspan="5">E = 60</td><td colspan="2">0.25</td><td>400</td></tr>
<tr><td>Rear Cushion (Helmet 1)</td><td colspan="5">E = 18</td><td colspan="2">0.25</td><td>200</td></tr>
<tr><td>OA Foams (Helmet 2)</td><td colspan="7">Direct compression data from experiment</td><td>164</td></tr>
<tr><td rowspan="2">Projectile</td><td>Cartridge Brass</td><td colspan="5">E = 110000</td><td colspan="2">0.375</td><td>8520</td></tr>
<tr><td>Lead Core</td><td colspan="5">G = 200</td><td colspan="2">-</td><td>11840</td></tr>
</table>

2.3 Failure Modeling of Helmet and FMJ Bullet

This preliminary study modeled both the helmet property degradation and the inter-laminar failure using surface traction criteria [Tan et al. (2012)]. Additionally, the Hashin Fabric Criterion was used to model the fabric-reinforced aramid laminates of the helmet shell which takes the bi-directional strength of the fibers into account [Tan et al. (2012)]. As for the FMJ bullet, Johnson Cook plasticity hardening and damage initiation criterion was used to model the exterior cartridge brass material [Johnson and Cook (1983)], whilst the Mie-Grüneisen hydrodynamic equation of state material model was used to model the lead core [Abaqus (2013)] (Table 2).

Table 2: Material constants in failure modeling of FMJ bullet.

Parts	Material Constants For Failure Modeling							
	Constants in Johnson-Cook Strain Rate Hardening							
	A	**B**	**n**	**M**	**T_m (K)**	**T_{trans} (K)**	**C**	**ε_0 (s^{-1})**
Cartridge Brass	112	505	0.42	1.68	1189	373	0.009	1
	Constants in Johnson-Cook Damage Initiation Criterion							
	d_1	**d_2**	**d_3**	**d_4**	**d_5**	**T_m (K)**	**T_{trans} (K)**	**ε_0 (s^{-1})**
	0.54	4.89	3.03	0.014	1.12	1189	373	1
Lead Core	**Constants in Mie-Grüneisen hydrodynamic equation of state (Linear Us-Up Hugoniot form)**							**Specific Heat Capacity ($J \cdot kg^{-1} \cdot K^{-1}$)**
	c_0 (cm/μs)		**s**			**Γ_0**		
	0.2006		1.429			2.60		150

2.4 Boundary Conditions

All the contact conditions imposed between the intracranial interfaces were taken from Tse et al. (2014). Table 3 shows the required boundary conditions of NIJ-STD-0106.00 that were applied at the base of the helmet-cushion-head assembly except for top impact which could be treated as if the military personnel proning on the ground while the fragment or bullet hits at the top of the helmet. As for initial condition, an initial velocity of $358 m \cdot s^{-1}$ was prescribed to the entire FMJ bullet [Aare and Kleiven (2007)], for each of the impact orientation and helmet cushions configuration.

Table 3: Boundary conditions for the NIJ ballistic impact simulations.

Impact Orientation	Displacement Constraints at the Base of the Helmet-Cushion-Head Assembly
Front	$U_2=0$; $U_3=0$; $\theta_1=0$; $\theta_3=0$
Side	$U_1=0$; $U_3=0$; $\theta_2=0$; $\theta_3=0$
Rear	$U_2=0$; $U_3=0$; $\theta_1=0$; $\theta_3=0$
Top	$U_1=0$; $U_2=0$; $U_3=0$; $\theta_3=0$

3. Results and Discussion

Table 4 showed the maximum values of the helmet strain, dynamic deflection as well as depth of helmet dent. The impact energy was partially absorbed by the helmet through deflection and deformation of the helmet shells, whilst majority of it was absorbed by the interior cushions. It could be seen in Table 4 that Helmet 1 generally deflected more than Helmet 2, except for lateral impacts. However, it should be noted that the projectile stroke on the rim of Helmet 1 with the presence of the underlying interior main loop preventing subsequent deflection, unlike the lateral impact of Helmet 2.

Table 4: Helmet parameters of the head with the two helmet configurations.

	Helmet 1 (with strap-netting)							
	Front	**Locations**	**Side**	**Locations**	**Rear**	**Locations**	**Top**	**Locations**
Max. Helmet Strain	0.195	Impact Site	0.164	Impact Site	0.039	Impact Site	0.120	Top Left of Helmet
Max. Dynamic Deflection (mm)	7.121	Right Helmet Rim	13.261	Right Helmet Rim	9.466	Left Helmet Rim	24.955	Left Helmet Rim
Max. Depth of Helmet Dent (mm)	10.452	Impact Site	12.597	Impact Site	12.628	Impact Site	13.624	Impact Site
Contact Between Helmet Shell & Head	No	-	No	-	No	-	No	-
	Helmet 2 (with OA foam padding)							
	Front	**Locations**	**Side**	**Locations**	**Rear**	**Locations**	**Top**	**Locations**
Max. Helmet Strain	0.074	Impact Site	0.105	Impact Site (2nd Outermost Layer)	0.037	Impact Site	0.0482	Posterior Top Right of Helmet
Max. Dynamic Deflection (mm)	5.911	Impact Site	28.569	Impact Site	6.665	Left Helmet Rim	16.846	Rear Helmet Rim
Max. Depth of Helmet Dent (mm)	10.817	Impact Site	15.185	Impact Site	9.665	Impact Site	12.566	Impact Site
Contact Between Helmet Shell & Head	No	-	No	-	No	-	No	-

Figure 2 showed the impact sequences of all the various orientations on the two helmets. Similar phenomenon had been observed in both helmets, as shown in Figure 2. It was noted that, in all eight impact orientation, there was no penetration of FMJ projectile into the helmets. This indicated that both the helmets had successfully deflected all the FMJ projectiles travelling at the speed of $358 m \cdot s^{-1}$ and met the NIJ requirement. In general, permanent dents of 9-15mm on the helmet exterior were observed at various sites of impact. The “crater” or spatial extent of the impression is around 60mm in diameter, and a bulge could be seen at the backplane of the helmet.

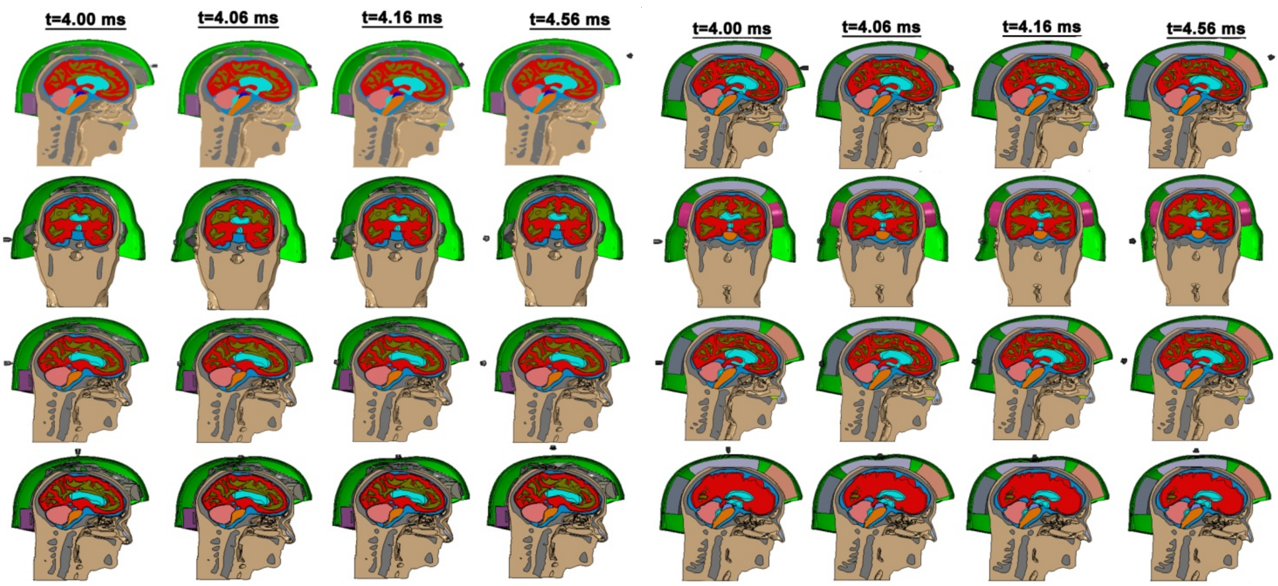

Figure 2: Impact sequence of various impact orientations for Helmet 1 (Left) and Helmet 2 (Right).

In this preliminary study, acceleration at the centre of the head was chosen as the parameter for analyses and for gauging the severity of TBI sustained (Figure 3). It was noted that the peak acceleration was found to be relatively high for both front and rear impacts for Helmet 1 (strap-netting) but were significantly reduced when equipped with Helmet 2 (OA foam). As for the remaining impact orientations (lateral and top impacts), Helmet 2 did not help much in reducing the peak head acceleration. Nevertheless, there was a general reduction in peak skull stresses in Helmet 2 (with OA foam padding) as compared to Helmet 1 (with strap-netting), with the percentage of reduction up to 44.94%, 0.07%, 109.21% and 8.39% for frontal, lateral, rear and top impacts. This showed that OA cellular foams were more effective as interior cushions as they limited the transmission of force by being able to absorb more energy, via plateau characteristic prior to foam densification, compared to the stiffer linear elastic front cushion of Helmet 1.

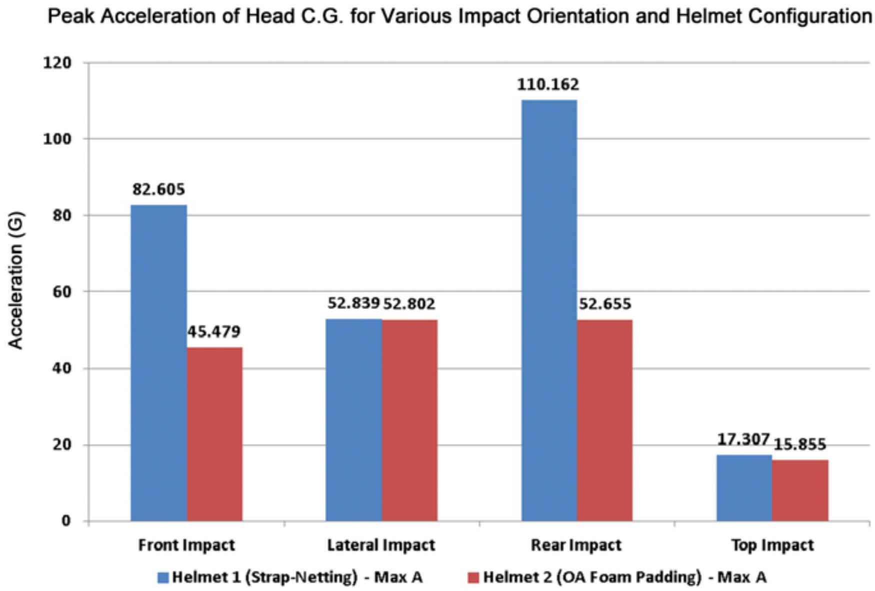

Figure 3: Peak acceleration at the C.G. of the head for various impact orientation and helmet liner configuration.

Comparison of the head acceleration obtained for various impact orientation indicated that the rear impact resulted in highest acceleration value of up to 110G when equipped with Helmet 1 (with strap-netting), followed by frontal and lateral impacts, whilst the lateral impact were most severe for Helmet 2 (with OA foam padding), followed by rear and front impacts. Top impacts were the least severe among all the impact orientation due to the nature of the boundary condition for the military personnel in the prone position. The peak acceleration values obtained from the simulations were also compared with the established injury criteria such as Wayne State Tolerance Curve (WSTC) and Federal Motor Vehicles Safety Standards (FMVSS) 218 criterion (Figure 4). It could be concluded from Figure 4 that all the impacts with both helmets passed the criteria of the WSTC and FMVSS.

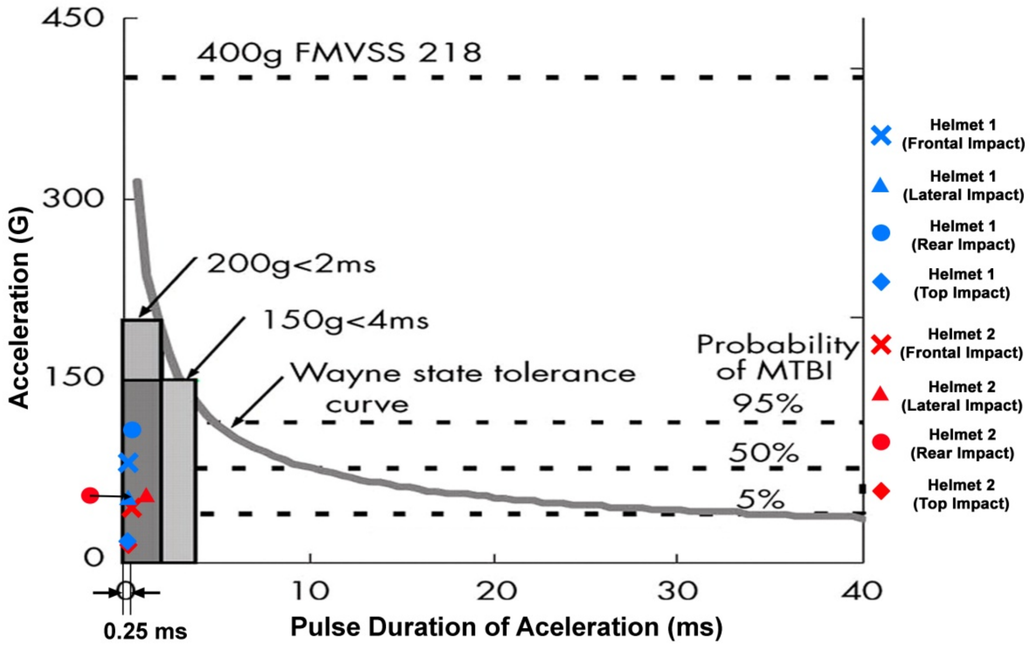

Figure 4: Acceleration responses for the helmets with two interior cushion designs in various impact directions, in relation to other published criteria Modified from [Shewchenko et al. (2005)].

4. Conclusion

In this study, ballistic analysis using FEM had been carried out to evaluate the performance of the ACH as well as the effectiveness of its interior cushioning systems, in protect both military personnel and civilians from traumatic head injury. Rear impacts gave rise to highest head acceleration while the top impacts were the least severe among all the impact orientation. The use of OA foams helped to reduce impact G forces and thus offered better protection from all various impact orientations. The simulations also showed both the helmets passed the NIJ requirement, WSTC and FMVSS criterion. However, it is still too early to arrive at any concrete conclusion for the severity of impact orientation since the human tolerance for different impact orientation was different [Allsop and Kennett (2002)] and the probability curves were based on automotive safety standards. More investigations on criterion for ballistic impact would be needed in the future.

Conflict of interest

None.

Acknowledgements

This work was supported by the Defence Science Organization (DSO) of Singapore. Special thanks to their researchers for providing the Advanced Combat Helmets (ACHs) and various interior cushioning systems. The authors would also like to acknowledge the National Natural Science Foundation of China (Grant No. 11272159).

References

Aare, M. and Kleiven, S. (2007). Evaluation of head response to ballistic helmet impacts using the finite element method, *International Journal of Impact Engineering* **34** (3), 596-608.

Abaqus Analysis User's Manual Version 6.13. Dassault Systèmes Simulia Corp.

Allsop, D. and Kennett, K. (2002). *Skull and facial bone trauma*. In: Nahum, A.M., Melvin, J. (Eds.), *Accidental Injury: Biomechanics And Prevention*. 2nd Edition. Springer-Verlag, pp. 577.

Baumgartner, D. and Willinger, R. (2003). Finite element modelling of human head injuries caused by ballistic projectiles. In: *Procceeding of NATO Research & Technology Organisation (RTO) Specialist Meeting*, Koblenz, Germany, 2003

Johnson, G.R. and Cook, W.H. (1983). A constitutive model and data for metals subjected to large strains, high strain rates and high temperature. In: *Procceeding of the 7th International Symposium on Ballistics*, 1983, 541-547.

Khalil, T.B. (1973). *Impact on a model head-helmet system*. University of California.

Khalil, T.B., Goldsmith, W. and Sackman, J.L. (1974). Impact on a model head-helmet system. *International Journal of Mechanical Sciences* **16** (9), 609-625.

Lee, H.P. and Gong, S.W. (2010). Finite element analysis for the evaluation of protective functions of helmets against ballistic impact. *Computer Methods in Biomechanics and Biomedical Engineering* **13** (5), 537-550.

National Institute of Justice (NIJ) Standard, NILECJ-STD-0106.00: Ballistic Helmets. 1975. ed. Justice, U.S.D.o. (Washington, DC, US).

Shewchenko, N., Withnall, C., Keown, M., Gittens, R. and Dvorak, J. (2005). Heading in football. Part 1: development of biomechanical methods to investigate head response. *Br J Sports Med* **39** Suppl 1, i10-25.

Tan, L.B., Tse, K.M., Lee, H.P., Tan, V.B.C. and Lim, S.P. (2012). Performance of an advanced combat helmet with different interior cushioning systems in ballistic impact: Experiments and finite element simulations. *International Journal of Impact Engineering* **50** (0), 99-112.

Tham, C.Y., Tan, V.B.C. and Lee, H.P. (2008). Ballistic impact of a KEVLAR® helmet: Experiment and simulations. *International Journal of Impact Engineering* **35** (5), 304-318.

Tse, K.M., Tan, L.B., Lee, S.J., Lim, S.P. and Lee, H.P. (2014). Development and validation of two subject-specific finite element models of human head against three cadaveric experiments. *International Journal for Numerical Methods in Biomedical Engineering* **30** (3), 397-415.

Van Hoof, J., Cronin, D.S., Worswick, M.J., Williams, K.V. and Nandlall, D. (2001). Numerical head and composite helmet models to predict blunt trauma. In: *Procceeding of 19th International Symposium on Ballistics, Interlaken, Switzerland*, 7-11 May 2001 2001

Van Hoof, J., Deutekom, M.J., Worswick, M.J. and Bolduc, M. (1999). Experimental and numerical analysis of the ballistic response of composite helmet materials. In: *Procceeding of 18th International Symposium on Ballistics*, San Antonio, TX, USA, 15-19 November 1999 1999

Yang, J. and Dai, J. (2010). Simulation-based assessment of rear effect to ballistic helmet impact. *Computer-Aided Design and Applications* **7** (1), 59-73.